Monthly Notices
of the
ROYAL ASTRONOMICAL SOCIETY

MNRAS **436,** 690–696 (2013)
Advance Access publication 2013 September 23

doi:10.1093/mnras/stt1606

B0707−359: a case study of change in AGN–black hole spin axis

L. Saripalli,[1]⋆ J. M. Malarecki,[2] R. Subrahmanyan,[1,3] D. H. Jones[4] and L. Staveley-Smith[2]

[1]*Raman Research Institute, C V Raman Avenue, Sadashivanagar, Bangalore 560080, India*
[2]*International Centre for Radio Astronomy Research, M468, The University of Western Australia, Crawley, WA 6009, Australia*
[3]*Science Operations Center, National Radio Astronomy Observatory, PO Box 0, Socorro, NM 87801, USA*
[4]*School of Physics, Faculty of Science, Monash University, Clayton, Victoria 3800, Australia*

Accepted 2013 August 22. Received 2013 August 22; in original form 2013 April 26

ABSTRACT

Structures of radio galaxies have the potential to reveal inconstancy in the axis of the beams, which reflect the stability in the spin axis of the supermassive black hole at the centre. We present radio observations of the giant radio galaxy B0707−359 whose structure offers an interesting case study of an active galactic nucleus (AGN) that may be exhibiting not only inconstancy in AGN output but also inconstancy in direction of ejection axis. Its radio morphology shows evidence for a restarting of the jets accompanied by an axis change. The observed side-to-side asymmetries of this giant radio galaxy suggest that the new jets are not in the plane of the sky. We infer that the hotspot advance velocities are unusually large and of magnitude a few tenths of the speed of light. The dual-frequency radio images are consistent with a model where the beams from the central engine ceased, creating a relic double radio source; this interruption was accompanied by triggering of a movement of the axis of the central engine at a rate of a few degrees Myr^{-1}. The closer location of the giant radio galaxy axis to the host minor axis rather than the host major axis is supportive of the restarting and axis-change model for the formation of the double–double structure rather than the backflow model.

Key words: galaxies: active – galaxies: individual: B0707−359 – galaxies: jets – radio continuum: galaxies.

1 INTRODUCTION

Giant radio galaxies (GRGs) and radio galaxies exhibiting evidence of restarted activity, the so-called 'double–double' radio galaxies are both testimony to the capability of jets and black hole spin axes to maintain long-term steadiness in their orientation. On the other hand, there has been evidence as well as several suggestions of precessing jets and of jets that might have flipped in orientation. Axis precession and flips may happen because of the influence of a nearby galaxy or as a consequence of a binary black hole merger (Ekers et al. 1978; Merritt & Ekers 2002; Campanelli et al. 2007). That jets can precess is already evident in the well-studied galactic microquasar SS 433 and inferred in radio galaxies such as 3C 123 (also 3C 294; Erlund et al. 2006). However, though simulations of binary black hole mergers have revealed that flips in jet axes are plausible mechanisms, there are few conclusive observational examples where an axis flip may have occurred (e.g. the triple double source 3C 293 (Akujor et al. 1996) and 4C+00.58 (Hodges-Kluck et al. 2010)). Detecting a flip in jet axis via morphology requires that the source be active along a previous axis for long enough time to have created extended lobes that survive as distinct relics that are visible in radio or X-ray images. Although morphologies of X-shaped radio galaxies may suggest occurrence of such an axis change there are several problems with this inference as being a general formation mechanism for this class of sources (Capetti et al. 2002; Saripalli & Subrahmanyan 2009; Hodges-Kluck & Reynolds 2011). Examples of radio galaxies with radio morphological evidence for changed axes between activity epochs are rare. More discoveries of potential examples where axes have changed over time are needed since they form a valuable resource for understanding the occurrence rate of perturbations to the black hole axes and for examining time-scales and conditions under which the axes change.

We present radio observations of the 1.10 Mpc GRG B0707−359 (redshift, $z = 0.1109$; Malarecki et al. 2013). The radio source is an unusual giant in that it represents a case of an active galactic nucleus (AGN) that appears to have restarted with a changed axis. We have imaged this source in the radio as part of a study of the ambient intergalactic medium using a sample of GRGs (Malarecki et al. 2013). We adopt a flat cosmology with Hubble constant $H_0 = 71\,\mathrm{km\,s^{-1}\,Mpc^{-1}}$ and matter density parameter $\Omega_\mathrm{m} = 0.27$.

⋆E-mail: lsaripal@rri.res.in

2 OBSERVATIONS AND RESULTS

The radio source was observed simultaneously at frequencies 1.4 and 2.3 GHz in several array configurations over several days using the Australia Telescope Compact Array (ATCA). A log of the observations is given in Table 1. The observations were carried out in total intensity and polarization. The observations of the source were interspersed with short 1.5–4 min observations of a suitable secondary calibrator B0727−365. The flux densities were set based on the known flux density of the primary calibrator B1934−638, which was observed once at the start of the observing run. The source was observed for a total of 53.4 h. Standard data reduction procedure was followed using MIRIAD in obtaining the final images. The data were phase self-calibrated to improve the imaging dynamic range. The final images are presented in Figs 1–3.

The total intensity maps at 1384 and 2368 MHz are shown in Figs 1 and 2; the radio morphology is a remarkable double–double structure: twin, very dissimilar lobe pairs that are skewed with respect to each other by as much as 30°. The outer lobe pair is asymmetric in extent from the centre and the lobes are dominated by bright hotspots at their ends. The second inner lobe pair is shorter in extent, diffuse and much fainter in surface brightness and quite symmetric about the core. These inner lobes are edge brightened; however, they show no evidence of hotspots in either lobe.

Table 1. Journal of ATCA observations at 1.4 and 2.3 GHz.

Array	Date	Time (h)
6C[a]	2000 November 11	9.09
1.5E[a]	2000 November 22	10.63
750C[a]	2000 December 29	9.68
375[a]	2001 February 27	10.27
750D	2004 June 14	3.79
6D	2004 December 07	9.98

[a]Observations with phase centre offset.

The polarization distributions are shown in both figures overlaid as vectors representing the electric field. The vectors have been corrected for Faraday rotation, which was estimated using the polarization data at 1384 and 2368 MHz. The polarization data reveal both pairs of lobes to be strongly polarized: the diffuse lobes have a mean percentage polarization between 10 and 20 per cent. In these lobe regions the projected magnetic field vectors are oriented parallel to the lobe edges.

Fig. 3 shows the spectral index distribution over the source. The spectral index distribution was computed using the 1384 MHz total intensity image and a separate low-resolution 2368 MHz image, which was produced from the calibrated data described above with the spatial frequency range truncated to a maximum of 28 $k\lambda$ so that the resulting image is matched in resolution to that of the 1384 MHz image. The limiting of the visibility coverage resulted in a reduction of the angular resolution from the 12 arcsec of Fig. 2 to 16 arcsec. The reduced resolution image was separately self-calibrated to improve the image dynamic range. The two-point spectral index map shows a generally steepening spectral index distribution towards the core region in the north-west (NW) inner lobe. The hotspots at the ends of the outer lobes have the expected flatter spectra. The core has an inverted spectrum ($S_\nu \propto \nu^\alpha$; $\alpha = 0.44$), which is not uncommon in radio galaxies (Slee et al. 1994).

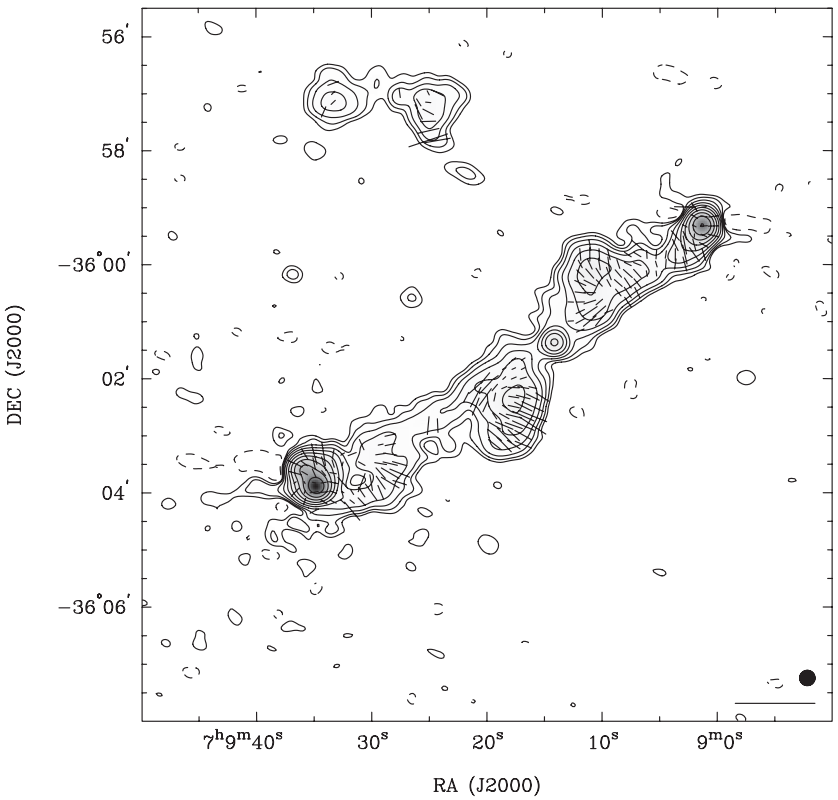

Figure 1. ATCA 1384 MHz radio continuum – primary beam-corrected, total intensity image with a beam of full width at half-maximum (FWHM) 16 arcsec and total intensity contours at −1, 1, 2, 4, 8, 16, 32, 64, 128 and 256 × 0.5 mJy beam^{-1}. Vectors corrected for Faraday rotation have been overlaid. The vectors represent fractional polarization (the scale bar represents 100 per cent polarization). Rms noise in the map is 0.16 mJy beam^{-1}.

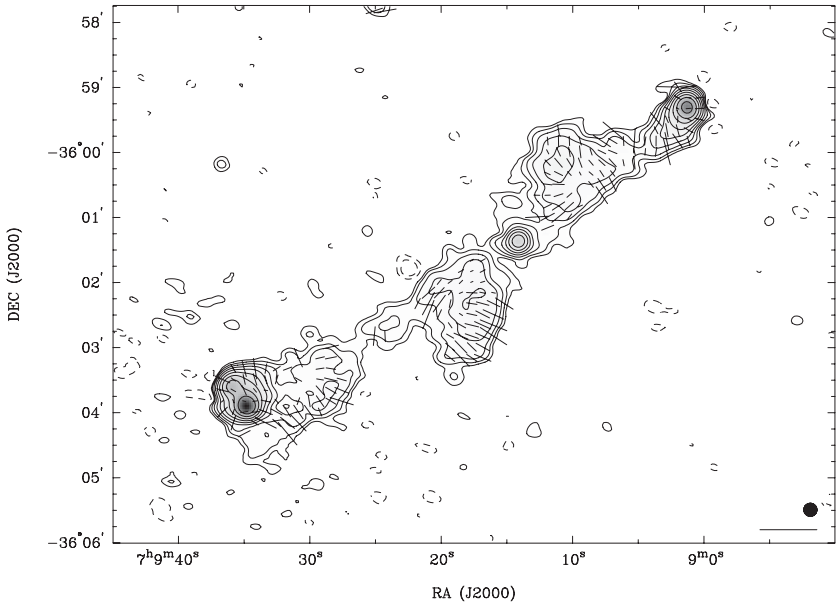

Figure 2. ATCA 2368 MHz radio continuum – primary beam-corrected, total intensity image with a beam of FWHM 12 arcsec and total intensity contours at −2, −1, 1, 2, 4, 8, 16, 32, 64, 128 and 256 × 0.4 mJy beam^{-1}. Vectors corrected for Faraday rotation have been overlaid. The vectors represent fractional polarization (the scale bar represents 100 per cent polarization). Rms noise in the map is 0.14 mJy beam^{-1}.

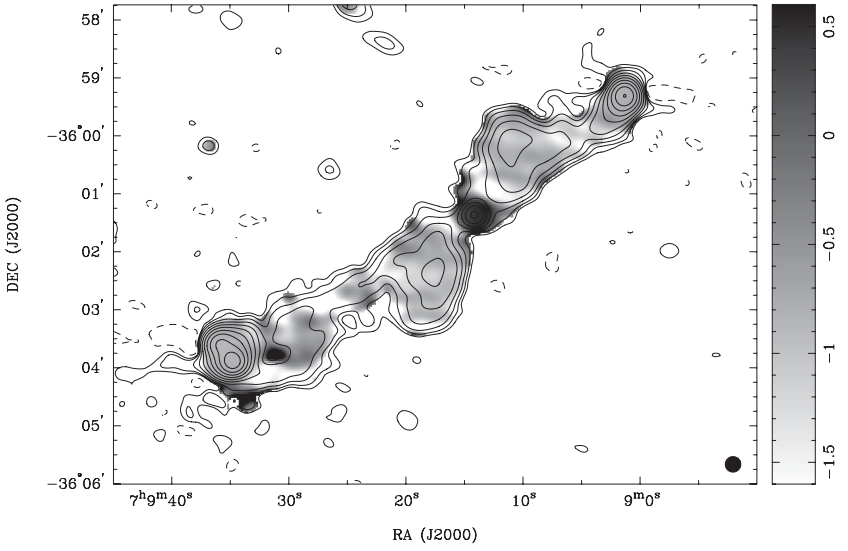

Figure 3. 20–13 cm spectral index distribution shown in grey-scale in the range −1.6 to +0.6 with a beam of FWHM 16 arcsec and overlaid with 1.4 GHz total intensity contours at −1, 1, 2, 4, 8, 16, 32, 64, 128 and 256 × 0.5 mJy beam^{-1}.

In Table 2 are listed some observed and derived properties for the source.

3 DISCUSSION

The relatively flat spectrum hotspots at the ends of the lobes are clearly the sites of termination shocks where jets from the centre currently end. The open question is the past evolution of the jets and their axes, which has implications for jet continuity and axis stability. Did the source experience an abrupt increase in hotspot advance speed, leaving behind the diffuse inner lobes and rapidly advancing to form the current hotspots? Do the inner lobes represent backflow of relativistic plasma from the sites of current hotspots, that are now along an axis offset from the current jet axis because the backflow has been deflected by the thermal halo associated with the host galaxy? Or do the inner lobes represent relic relativistic plasma that was deposited at their current sites by jets that were along the axis of the inner lobes in a previous epoch of activity? In the subsections below we consider these alternatives in the light of the observations presented here.

The GRG has prominent hotspots at the ends and has lobes that remain relatively narrow over some distance towards the core before flaring in opposite directions. The NW and south-east (SE) inner regions may be interpreted as flared parts of the radio lobes, which are recessed and confined to the vicinity of the core, with the outer regions viewed as protuberances. In this picture, the lobes on both sides have a bottleneck appearance. Such a morphology has been observed in several prominent 3C radio galaxies (e.g. 3C 33,

Table 2. Source properties at 1.4 and 2.3 GHz.

Properties of the core	1.4 GHz	2.3 GHz
Integrated flux density (mJy)	44.6	53.0
Spectral index[a] ($S_\nu \propto \nu^\alpha$)	0.44	
Properties of the offset inner double	1.4 GHz	2.3 GHz
Total flux [incl. core] (Jy)	0.49	0.33
Power (W hz^{-1}) [in the rest frame of the source]	1.64×10^{25}	1.10×10^{25}
Mean spectral index in N lobe[a]	−0.89	
Mean spectral index in S lobe[a]	−0.99	
Mean fractional polarization for the N lobe (per cent)	12.4	17.9
Depolarization ratio for the N lobe	0.69	
Mean fractional polarization for the S lobe (per cent)	17.1	21.9
Depolarization ratio for the S lobe	0.78	
Mean rotation measure in N lobe (rad m^{-2})	58.0	
Mean rotation measure in S lobe (rad m^{-2})	62.4	
Pressure of the N lobe (outer region) (Pa)	2.03×10^{-14}	
Pressure of the S lobe (outer region) (Pa)	1.79×10^{-14}	
Properties of the outer double	1.4 GHz	2.3 GHz
Total flux [incl. core] (Jy)	1.50	0.98
Power (W hz^{-1}) [in the rest frame of the source]	5.05×10^{25}	3.31×10^{25}
Spectral index at the N hotspot[a]	−0.80	
Spectral index at the S hotspot[a]	−0.83	
Lobe extent asymmetry	1.47	
Mean rotation measure in N lobe (rad m^{-2})	60.3	
Mean rotation measure in S lobe (rad m^{-2})	63.3	

[a]Indicates all spectral index values have been calculated using 16 arcsec images at both 1.4 and 2.3 GHz.

3C 79, 3C 132, 3C 184.1, 3C 234, 3C 349, 3C 381 and 3C 390.3). Such sources with protruding hotspots have been speculated to form because of either a sudden drop in the ambient medium density or sudden increase in the jet density or power or in the steadiness of the beam (Leahy & Perley 1991; Hardcastle et al. 1997); these circumstances result in a step increase in advance speed of the hotspot.

As we trace the outer lobes from the hotspots towards the core, the flaring in the form of the inner lobes first occurs at similar distances of about 250 kpc from the core. These flared regions are very similar in appearance and extend in opposite directions. They are collinear with the core forming an axis which is offset from the axis defined by the hotspots by an angle of about 30°. They are both well bounded at their leading ends and have projected magnetic field vectors that run parallel to the edges. All these characteristics of the flared regions suggest a resemblance in several respects to radio lobes rather than the central flares and distortions seen in radio galaxies (Leahy & Williams 1984; Saripalli & Subrahmanyan 2009). The two emission regions also appear to lack compact features and they have a relaxed appearance with relatively low axial ratios.

The GRG B0707−359 displays a structure that has both inversion symmetry and a marked offset between the outer and inner lobes. Any explanation proffered for the radio structure we observe in B0707−359, whether in terms of a sudden drop in the ambient medium density or sudden increase in the jet density or power or in the steadiness of the beam, will need to take into account the offset in axes between the inner and outer lobes.

3.1 Is the structure in B0707−359 caused by abrupt changes in ambient medium?

For an abrupt change in density of the ambient medium to be responsible for the narrow protrusions of the two outer lobes, the density change will not only have to occur at the large distance of nearly 250 kpc from the host galaxy but the change will need to be such that it also deflects the two jets inversion symmetrically in opposite directions. While density changes in the associated thermal haloes of elliptical galaxies may occur symmetrically on both sides, they are unlikely to occur at such large distance from the host. The change in ambient density is also required to occur at more than twice the distance over which bottleneck structures are observed to appear in the other examples known in the literature. More significantly, the lack of abrupt bends in the two outer lobes (suggestive of deflection as they emerge out of the inner lobes) and the common axis they appear to share pose a difficulty for this model. It is more likely that changes in jet properties instead may be responsible for the peculiar structure of B0707−359: either an increase in jet density (hence power) or in its steadiness, accompanied also by a change in the axis of the jets.

3.2 Is the structure in B0707−359 caused by deflection of backflows?

Deflection of backflows in a thermal medium associated with the host galaxy has been suggested as a mechanism by which inversion symmetric central distortions in radio galaxies (type-2 distortion; Leahy & Williams 1984, fig. 6a) as well as the 'wings' in X-shaped radio galaxies (XRGs) may be produced (e.g. Leahy & Williams 1984; Worrall et al. 1995). Could the same physical process also be responsible for the offset inner lobes in B0707−359? Given the presence of prominent hotspots at the ends of the outer lobes strong backflows are expected. However, the backflows appear to stop well short of the core and instead deviate from the main axis at scales of more than 200 kpc from the core on either side. This is in sharp contrast to the features commonly seen as central lobe distortions in samples of radio galaxies or the wings in XRGs. Moreover, the two inner lobes in B0707−359 as already described are edge brightened, well-bounded emission regions offset at a relatively small angle with respect to the main radio axis all of which also

contrast with properties associated with commonly seen distortions in radio galaxies or XRGs. Given the strong differences the thermal halo may not have a major influence on the backflows.

In the context of the reported geometrical relationship between the host optical axes and radio axes of radio galaxies (Capetti et al. 2002; Saripalli & Subrahmanyan 2009) where radio galaxies with both prominent central distortions and XRGs were found to predominantly lie closer to the host major axes it would be revealing to examine the relative orientations in B0707−359. Given the arguments presented against backflow deflection mechanism in the formation of the offset structures in B0707−359 such a major-axis orientation of the radio axis is not expected. Instead, given the propensity of GRGs to lie with their radio axes closer to the host minor axes (Saripalli & Subrahmanyan 2009) it suggests a minor-axis orientation for B0707−359.

Using available data we have estimated the major axis position angle of the host galaxy. GALFIT (version 3.0.5) was used to fit the image of the B0707−359 optical host detected in Digitized Sky Survey (DSS; red), Two Micron All-Sky Survey (2MASS) and *Swift* (*V*-band) data. Four *Swift V*-band data sets were summed to form a single image, with a combined exposure time of 1117 s, using the HEASOFT programs UVOTIMSUM and XIMAGE. For each image, the plate scale in arcsec pixel^{-1} and photometric zero-point were set, and the sky background in the fitting region in analog-to-digital units (ADUs) and integrated magnitude for the host were estimated. The position angle of the host elliptical galaxy (as measured by GALFIT in degrees from north through east) is 78, 82 and 72 using the DSS, 2MASS and *Swift* data, respectively. While in all the data sets the host galaxy counts may be affected by light from a nearby bright star to the east, the 2MASS image has a relatively poor signal-to-noise ratio and may be less reliable. The derived major axis position angle (offset by nearly 55° with respect to the outer double radio axis, considering DSS and *Swift* data) agrees (1) with our reasoning above against formation of the offset lobes as a result of backflow deflection (where the radio axis is expected to be located closer to major axis) and (2) with the expectation of a closeness with host minor axis for the axes of GRGs (Saripalli & Subrahmanyan 2009).

3.3 Has there been an axis flip in B0707−359?

The more simplistic scenario for the source structure we observe in B0707−359 is that the source may have experienced a flip in the jet axis between two epochs of activity. The source was initially active along the direction of the inner lobes and the jet activity then switched off for a period of time after which it again became active but along a different direction that is offset by about 30° to the NW. Restarting – the switching off and switching back on of the AGN beams – in radio galaxies is today a well accepted model that has been established to occur in several cases and has accumulated much support over the years (Bridle, Perley & Henriksen 1986; Roettiger et al. 1994; Akujor et al. 1996; Subrahmanyan, Saripalli & Hunstead 1996; Schoenmakers et al. 2000; O'Dea et al. 2001; Saripalli, Subrahmanyan & Udayashankar 2002, 2003; Saripalli et al. 2005, 2012; Marecki et al. 2006; Saikia, Konar & Kulkarni 2006; Brocksopp et al. 2007; Jamrozy et al. 2007; Jamrozy, Saikia & Konar 2009; Marecki & Szablewski 2009; Blundell & Fabian 2011; Giancintucci et al. 2012). Additional evidence comes from the examples of and formation scenarios for multiple pairs of X-ray 'holes' associated with AGN at the centres of galaxy clusters and groups (McNamara & Nulsen 2007).

Our two-frequency spectral index distribution unfortunately does not allow a clear picture to emerge. If the two inner lobes are the relics of past activity, not only should they have steeper spectral indices compared to the rest of the source, they should also have spectral gradients with steeper spectral indices towards the central regions. Both inner lobes do have steeper spectral indices on average than the outer lobes, although only −0.9 compared to −0.8 in the outer lobes. However, the spectral index distribution (Fig. 3) does not clearly show the expected steepening towards the central regions; while NW inner lobe may have such a trend, such a behaviour is not apparent in the case of the SE inner lobe. Regions of flatter indices are noticed in both the inner lobes along the main radio axis (formed by the outer hotspots) possibly indicating influence of younger jet material associated with the outer lobes. Whereas further away from the common emission regions of both NW and SE inner lobes prominent areas of steep spectral indices of −1 to −1.2 are indeed seen.

The source morphology, polarization structure and to a lesser extent the spectral index distribution are all consistent with the likelihood of a restarting of activity in this source where the new jets have emerged along a changed direction. We also note here that the integrated radio power of the inner lobe pair alone (Table 1) is comparable to that of radio galaxies, being close to the dividing line between edge-brightened and edge-darkened radio galaxies. Here we pause and ask whether the inner double, with its low lobe axial ratio, lack of hotspots in an edge-brightened structure and circumferential magnetic fields, may instead be a lobed Fanaroff–Riley I (FR-I) like 3C 296 or NGC 326 rather than being the relic of a previous Fanaroff–Riley II (FR-II) episode (and hence suggesting instead an axis change from outer to inner double). This possibility however is less likely because of absence of prominent twin jets found ubiquitously in FR-I sources. Taken together with the short lifetimes of hotspots seen in the outer double (few 10^4 yr) and the age of the weaker episode (powered by slower jets), the inner double is unlikely to be a lobed FR-I. This is supportive of the jets initially being located along the position angle of the inner double and then rotating to the axis of the outer double.

A change in the direction of the jets when restarting in a new epoch is not common. Most examples of radio galaxies with restarted activity show jet axes that have remained unchanged. The few examples where a changed jet direction is recognized are the well known triple–double source 3C 293 (Akujor et al. 1996) and the more recent example of 4C+00.58 (Hodges-Kluck et al. 2010). In these examples the emission regions corresponding to the two epochs are distinct whether in morphology or physical separation or stage of activity (e.g. in 3C 293) lending a strong case for change of axis after a switching off of the central beams.

The morphology of the older epoch emission will depend on the time for which the jets have remained switched off (the quiescent time). In B0707−359, if indeed the inner pair of lobes represent older activity, the quiescent time may not have been long because the lobes are well bounded over their 250 kpc extent although they lack hotspots and have low axial ratios. Using an equipartition magnetic field of about 2.5 μG (Malarecki et al. 2013) for the inner lobes and the fact that the break frequency is above 2.3 GHz the upper limit to the source age is derived to be 10^8 yr.

A pronounced asymmetry (of 1.47) is seen for the outer lobes which is not seen for the inner pair. Because of the rather similar appearance and symmetric extent of the inner lobe pair, we may expect that there is little asymmetry in the properties of the external medium over a distance of at least 250 kpc from the host galaxy. For the environment to be responsible for the asymmetry in the extents of the outer lobes, the medium on scales larger than 250 kpc must be asymmetric. While this is possible, we discuss below an

alternate and more likely origin for the asymmetric appearance. The available optical images are not of sufficient quality to assess the neighbouring galaxy environment. This is being studied as part of a separate program involving a larger sample of GRGs.

The alternate origin for the asymmetric appearance of the outer lobes involves light travel time effects. It is likely that the new and current jet axis is not in the plane of the sky. A current jet axis with the approaching side towards the SE will result in a longer extent for that lobe compared to the opposite NW side because of light travel time effects. For inclined jets to give rise to a pronounced asymmetry the advance speeds of the hotspots will need to be relativistic. The optical spectrum of the host galaxy does not show broad emission lines (Malarecki et al. 2013), which suggests that the axis of the AGN is inclined by more than 45° to the line of sight. To produce the observed asymmetry of 1.47 in the ratio of the apparent projected lengths of the two outer lobes, a head advance speed of at least $0.27c$ is necessitated by the constraint on the inclination angle: larger and unrealistic advance speeds are required to explain the asymmetry ratio if the inclination angle is much greater than 45°. This argues for an inclination angle close to 45° along with advance speed close to $0.3c$. It is possible however that the AGN lacks a broad-line region altogether. In such a case the constraint on the inclination angle is relaxed to allow angles smaller than 45° and the head advance speeds required will be lower, although still remaining relatively high.

The rather high advance speeds of the ends of the outer lobes suggest a relatively young age of 6 Myr for the Mpc-size outer double. Additionally, it may be noted that such high advance speeds have rarely been inferred for jets interacting with the ambient intergalactic medium: it is instead in the case of hotspots linked with restarting jets advancing in relic cocoons that such large advance speeds have been suggested (Safouris et al. 2008).

This model also expects that the approaching hotspot would have an increased flux density compared to the receding hotspot because of relativistic beaming of the hotspot emissions. However, for inclination angles close to 45° along with advance speeds close to $0.3c$ the expected hotspot flux ratio is 4.3, which is well above the observed ratio of 1.6 (ratio of the brighter peak in the SE lobe to the NW hotspot peak).

Here we point to the curious non-collinearity of the hotspots in the two outer lobes with the core as well as the multiple hotspots observed at the SE end. The SE hotspots are displaced to the east with respect to the axis formed by the core and the NW hotspot. This is in the same direction as that suggested above for the axis flip of 30° from the direction of the inner offset lobes to the outer lobes. We may understand the angular offsets between the inner relic double and the outer hotspots, as well as the offsets between the hotspots at the two outer ends, by a model that invokes a clockwise rotation of the axis of the radio jets over time.

From the angle of non-collinearity of about 10° between the NW and SE outer hotspots and the light travel time difference of nearly 2.5 Myr required to produce the seen asymmetry in extents of the two outer lobes we infer a clockwise rotational speed of about $4^\circ\ \mathrm{Myr}^{-1}$ for the ejection axis of the radio jets. In this model that invokes episodic jets along with a rotating ejection axis, the inner double was created at an earlier epoch and is observed today as relic lobes defining that past axis orientation. Subsequently the axis rotated and a new activity episode resulted in the observed hotspot at the NW end and a corresponding hotspot along that axis to the SE. A southern extension from the current SE hotspot (Fig. 2) might be the remnant of that SE hotspot. Continued episodic activity as the axis continued to rotate clockwise resulted in the bright hotspot at the SE end; the counterpart of this activity is yet to be observed at the NW end owing to light travel time delay in that receding lobe.

This brightest hotspot in SE end is currently diminished in brightness because the jet in that lobe is already moving on to feed another hotspot at an advanced rotation angle; this sharing of the beam power may be a reason for this SE hotspot to be fainter compared to the expectations derived above for the inclination angle and advance speed. Additionally, since the sound crossing time for a 1 kpc hotspot is expected to be only 10^4 yr, the hotspot flux will be variable on that time-scale unless the beam is stationary in power and orientation. For these reasons, it is difficult to relate the hotspot flux ratio to the Doppler factor.

In the model proposed above the black hole spin axis rotates at a speed of $4^\circ\ \mathrm{Myr}^{-1}$ and at this speed it would have taken about 7 Myr to change from the direction of the inner relic double to the axis defined by the outer bright hotspots. Adding to this the dynamical age of the giant radio source, we infer that the relic inner lobes are at least 13 Myr old. This is consistent with the upper limit of 10^8 yr derived above for the age of the inner double.

The 14–195 keV X-ray luminosity reported for the source identified with the B0707−359 host galaxy in the *Swift*/Burst Alert Telescope (BAT) hard X-ray survey allows us to compare with the kinetic luminosity in the jets of the GRG as a consistency check for the scenario considered above (that the active jets are presently oriented along the GRG and the source may be growing with a high advance speed of $0.3c$). We use the equipartition pressure derived for the inner lobes (we assume the same in the extended regions of the outer lobes) together with the dimensions of the outer lobes (625 kpc for the SE lobe and 440 kpc for the NW lobe with a common width and depth of 100 kpc) and the estimated age for the GRG of 6 Myr to derive a jet kinetic luminosity of $1.9 \times 10^{44}\ \mathrm{erg\ s}^{-1}$ (for the SE jet) and $1.3 \times 10^{44}\ \mathrm{erg\ s}^{-1}$ (for the NW jet). These values compare well with the (14–195 keV) hard X-ray luminosity of $4.8 \times 10^{44}\ \mathrm{erg\ s}^{-1}$ for the AGN.

Some aspects of the scenario sketched above that we did not address are what causes the jets to rotate between the jets forming the relic lobes and the jets beginning to drive lobes in new directions and whether the jets could have been active throughout the rotation instead of discrete activity episodes that created the inner and outer lobe pairs. Dennett-Thorpe et al. (2002) discuss the causes of jet axis rotation that include on one hand change in accretion disc angular momentum (e.g. due to gas driven by minor merger) as the primary cause and on the other hand change in black hole axis (due to a past major merger) being the main driver. In either case the visible signs of the past events may not be strong and the estimated time-scales for the jet axis rotation can range from half Myr to 10^7 yr. As for the continued jet activity during the rotation, we cannot rule out the possibility and instead there may be some support for it in the form of lack of clear trends as well as shallower than expected inner lobe spectral index distribution. Clearly, in the morphology of GRG B0707−359, we may be witnessing a consequence of jet rotation. Time-scales, causes and effect on AGN activity all need to be further understood. B0707−359 may be a good candidate to explore these aspects of AGN physics.

In an altogether different scenario to explain the source structure there is the possibility that the inner and outer lobe pairs represent manifestations of two separate but close AGN whose axes are offset from each other (Lal & Rao 2007). As yet however there has been no convincing case of such a close pair of AGN both of which are also radio galaxies (3C 75 known for its dual radio source structure has AGN cores that are separated by more than 7 kpc). There are several studies and programs however that are attempting to identify

cases of close pairs of supermassive black holes and a few strong candidates have been reported where there are two milli-arcsecond radio cores (Rodriguez et al. 2006; Frey et al. 2012).

In the study of the extended structure in GRG B0707−359 presented here a few tests will be interesting and useful to carry out. For example if the inner double is indeed a relic source mapping it with higher resolution is not expected to reveal bright jets. Again, if the radio jet is aligned 45° to the line of sight then we expect in a high-resolution optical/IR observation to see presence of broad emission lines in polarized flux. Also it will be useful to carry out very long baseline interferometry (VLBI) observations of the core to check for presence of twin cores which are expected if the peculiar structure is because of two nearby AGN.

4 SUMMARY

We have presented radio continuum observations in total intensity and polarization of the GRG B0707−359. The source has an unusual morphology in that two radio lobe pairs are recognized which are offset from each other at an angle of 30°. Not only that there are two lobe pairs and that they are offset from each other, the new lobes are both of bottleneck nature and protrude well out of the 250 kpc inner lobes to different distances. We have tried to understand how the source structure may have formed and we have presented arguments that lead to an internally consistent scenario for the formation of the source morphology as that of an AGN which has restarted its jets with the new and current jets propagating in a direction different from the original jets. We infer that the AGN has restarted its jets in an offset direction; moreover, we also infer that the new direction is not in the plane of the sky. The location of the GRG axis defined by the hotspots, along an angle closer to the host minor axis rather than the major axis, supports a restarting and axis-change model for the formation of the structure we see in B0707−359. It is also consistent with a previous study suggesting a preference for GRGs to develop closer to host minor axes (Saripalli & Subrahmanyan 2009).

ACKNOWLEDGEMENTS

ATCA is part of the Australia Telescope, which is funded by the Commonwealth of Australia for operation as a National Facility managed by CSIRO. This publication makes use of data products from the Two Micron All Sky Survey, which is a joint project of the University of Massachusetts and the Infrared Processing and Analysis Center/California Institute of Technology, funded by the National Aeronautics and Space Administration and the National Science Foundation. The Digitized Sky Surveys were produced at the Space Telescope Science Institute under U.S. Government grant NAG W-2166. The images of these surveys are based on photographic data obtained using the Oschin Schmidt Telescope on Palomar Mountain and the UK Schmidt Telescope. The plates were processed into the present compressed digital form with the permission of these institutions. This research has also made use of data obtained through the High Energy Astrophysics Science Archive Research Center Online Service, provided by the NASA/Goddard Space Flight Center. We thank the anonymous referee for very helpful suggestions which have improved the paper.

REFERENCES

Akujor C. E., Leahy J. P., Garrington S. T., Sanghera H., Spencer R. E., Schilizzi R. T., 1996, MNRAS, 278, 1
Blundell K. M., Fabian A. C., 2011, MNRAS, 412, 705
Bridle A. H., Perley R. A., Henriksen R. N., 1982, AJ, 92, 534
Brocksopp C., Kaiser C. R., Schoenmakers A. P., de Bruyn A. G., 2007, MNRAS, 382, 1019
Campanelli M., Carlos L., Zlochower Y., Merritt D., 2007, ApJ, 659, L5
Capetti A., Zamfir S., Rossi P., Bodo G., Zani C., Massaglia S., 2002, A&A, 394, 39
Dennett-Thorpe J., Scheuer P. A. G., Laing R. A., Bridle A. H., Pooley G. G., Reich W., 2002, MNRAS, 330, 609
Ekers R. D., Fanti R., Lari C., Parma P., 1978, Nat, 276, 588
Erlund M. C., Fabian A. C., Blundell K. M., Celotti A., Crawford C. S., 2006, MNRAS, 371, 29
Frey S., Paragi Z., An T., Gabanyi K. E., 2012, MNRAS, 425, 1185
Giacintucci S. et al., 2012, ApJ, 755, 172
Hardcastle M. J., Alexander P., Pooley G. G., Rley J. M., 1997, MNRAS, 288, 859
Hodges-Kluck E. J., Reynolds C. S., 2011, ApJ, 733, 58
Hodges-Kluck E. J., Reynolds C. S., Coleman Miller M., Cheung C. C., 2010, ApJ, 717, L37
Jamrozy M., Konar C., Saikia D. J., Stawarz L., Mack K.-H., Siemiginowska A., 2007, MNRAS, 378, 581
Jamrozy M., Saikia D. J., Konar C., 2009, MNRAS, 399, 141
Lal D. V., Rao A. P., 2007, MNRAS, 374, 1085
Leahy J. P., Perley R. A., 1991, AJ, 102, 537
Leahy J. P., Williams A. G., 1984, MNRAS, 210, 929
McNamara B. R., Nulsen P. E. J., 2007, ARA&A, 45, 117
Malarecki J. M., Staveley-Smith L., Saripalli L., Subrahmanyan R., Jones D. H., Duffy J. R., Rioja M., 2013, MNRAS, 432, 200
Marecki A., Szablewski M., 2009, A&A, 506, 33
Marecki A., Thomasson P., Mack K.-H., Kunert-Bajraszewska M., 2006, A&A, 448, 479
Merritt D., Ekers R. D., 2002, Sci, 297, 1310
O'Dea C. P., Koekemoer A. M., Baum S. A., Sparks W. B., Martel A. R., Allen M. G., Macchetto F. D., Miley G. K., 2001, AJ, 121, 191
Rodriguez C., Taylor G. B., Zavala R. T., Peck A. B., Pollack L. K., Romani R. W., 2006, ApJ, 646, 49
Roettiger K., Burns J. O., Clarke D. A., Christiansen W. A., 1994, ApJ, 421, 23
Safouris V., Subrahmanyan R., Bicknell G. V., Saripalli L., 2008, MNRAS, 385, 2117
Saikia D. J., Konar C., Kulkarni V. K., 2006, MNRAS, 366, 1391
Saripalli L., Subrahmanyan R., 2009, ApJ, 695, 156
Saripalli L., Subrahmanyan R., Udayashankar N., 2002, ApJ, 565, 256
Saripalli L., Subrahmanyan R., Udayashankar N., 2003, ApJ, 590, 181
Saripalli L., Hunstead R. W., Subrahmanyan R., Boyce E., 2005, AJ, 130, 896
Saripalli L., Subrahmanyan R., Thorat K., Ekers R. D., Hunstead R. W., Johnston H. M., Sadler E. M., 2012, ApJS, 199, 27
Schoenmakers A. P., de Bruyn A. G., Roettgering H. J. A., van der Laan H., 2000, MNRAS, 315, 395
Slee O. B., Sadler E. M., Reynolds J. E., Ekers R. D., 1994, MNRAS, 269, 928
Subrahmanyan R., Saripalli L., Hunstead R. W., 1996, MNRAS, 279, 257
Worrall D. M., Birkinshaw M., Cameron R. A., 1995, ApJ, 449, 93

This paper has been typeset from a TEX/LATEX file prepared by the author.